


Density of tertiary lymphoid structures predicts clinical outcome in breast cancer brain metastasis

Yuan-Yuan Zhao,¹ Zhen Fan ,^{2,3,4,5,6,7} Bao-Rui Tao,¹ Zun-Guo Du,⁸ Zhi-Feng Shi^{2,3,4,5,6,7}

To cite: Zhao Y-Y, Fan Z, Tao B-R, *et al.* Density of tertiary lymphoid structures predicts clinical outcome in breast cancer brain metastasis. *Journal for ImmunoTherapy of Cancer* 2024;**12**:e009232. doi:10.1136/jitc-2024-009232

► Additional supplemental material is published online only. To view, please visit the journal online (<https://doi.org/10.1136/jitc-2024-009232>).

Y-YZ, ZF and B-RT contributed equally.

Accepted 10 July 2024

ABSTRACT

Background Patients with breast cancer brain metastases (BCBM) experience a rapid decline in their quality of life. Recently, tertiary lymphoid structures (TLSs), analogs of secondary lymphoid organs, have attracted extensive attention. However, the potential clinical implications of TLSs in BCBMs are poorly understood. In this study, we evaluated the density and composition of TLSs in BCBMs and described their prognostic value.

Methods Clinicopathological data were collected from 98 patients (2015–2021). TLSs were evaluated, and a TLS scoring system was constructed. Differences in progression-free survival (PFS) and overall survival (OS) between groups were calculated using the Kaplan-Meier method. Immunohistochemistry and multiplex immunofluorescence (mIF) were used to assess TLSs heterogeneity.

Results TLSs were identified in 47 patients with BCBM. High TLSs density indicated favorable survival (OS, $p=0.003$; PFS, $p<0.001$). TLS was positively associated with OS ($p=0.0172$) and PFS ($p=0.0161$) in the human epidermal growth factor receptor type 2-positive subtype, and with prolonged OS ($p=0.0482$) in the triple-negative breast cancer subtype. The mIF results showed significant differences in the percentages of T follicular helper (Tfh) cells, M2 macrophages, cytotoxic T lymphocytes, and CD8⁺TIM-3⁺ T lymphocytes between the groups of TLS scores 0–3 (cytotoxic T lymphocytes, $p=0.044$; Tfh, $p=0.021$; M2 macrophages, $p=0.033$; CD8⁺TIM-3⁺ T lymphocytes, $p=0.018$). Furthermore, novel nomograms incorporating the TLS scores and other clinicopathological predictors demonstrated prominent predictability of the 1-year, 3-year, and 5-year outcomes of BCBMs (area under the curve >0.800).

Conclusion Our results highlight the impact of TLSs abundance on the OS and PFS of patients with BCBM. Additionally, we described the immune composition of TLSs and proposed novel nomograms to predict the prognosis of patients with BCBM.

INTRODUCTION

Brain metastasis (BrM) commonly occurs in patients with solid tumors, is associated with poor survival outcomes and presents considerable complexities in clinical management. Breast cancer (BC) ranks second among solid malignancies involving the brain, following

WHAT IS ALREADY KNOWN ON THIS TOPIC

⇒ Brain metastases commonly occur in patients with breast cancer, are associated with poor survival outcomes and present considerable complexities in clinical management. Tertiary lymphoid structure (TLSs) are analogous to secondary lymphoid organs and have gained widespread attention. However, the potential clinical implications and underlying mechanisms of TLSs in breast cancer brain metastase (BCBM) patients are poorly understood.

WHAT THIS STUDY ADDS

⇒ TLSs have been identified in breast cancer brain metastases, but have not been previously reported in the literatures. The majority of TLSs in BCBM exhibited characteristics of early TLSs (dense lymphocytic aggregates with mixed B and T cells without CD21 or CD23 expression). Our comprehensive assessment of TLSs in BCBM sheds light on the interaction between TLSs density and prognosis, demonstrating its prognostic role according to breast cancer subtype and differences in immune composition. We also found significant differences in the percentages of T follicular helper cells, M2 macrophages, cytotoxic T lymphocytes, and CD8⁺TIM-3⁺ T lymphocytes between groups with different TLS scores.

HOW THIS STUDY MIGHT AFFECT RESEARCH, PRACTICE OR POLICY

⇒ This study emphasizes the prognostic values of TLSs in BCBM and explores the heterogeneous immune composition, with the ultimate purpose of identifying biological targets and informing future clinical trials.



© Author(s) (or their employer(s)) 2024. Re-use permitted under CC BY-NC. No commercial re-use. See rights and permissions. Published by BMJ.

For numbered affiliations see end of article.

Correspondence to

Dr Zhen Fan;
zhenfan@fudan.edu.cn

Professor Zhi-Feng Shi;
shizhifeng@fudan.edu.cn

lung cancer.¹ Despite improved disease control and overall survival (OS), 15%–30% of patients with BC develop BrM.² Patients with BC brain metastasis (BCBM) experience progressive neurological functional deficits and a rapid decline in their quality of life. Notably, BrM tends to occur in aggressive BC subtypes, such as the human epidermal growth factor receptor type 2 (HER2)-positive and triple-negative BC (TNBC) subtypes,^{1,3} which are also usually considered more immunogenic, harbor greater amounts

of tumor-infiltrating lymphocytes, and have a better immune response.⁴

The brain is commonly regarded as a sanctuary for cancers because of its immune-specialized nature and immune-privileged status.⁵ Nevertheless, emerging data have confirmed the activity of immunotherapeutic agents in patients with melanoma and lung cancer with BrM.⁶ Importantly, the composition of the tumor microenvironment (TME) correlates with the patient response to immunotherapy in multiple cancers.^{7,8} Tertiary lymphoid structures (TLSs), also known as ectopic lymphoid tissues, have recently attracted considerable attention. TLSs are considered analogs of secondary lymphoid organs and develop in non-lymphoid tissues at sites of tumors, autoimmune diseases, or infectious diseases.^{9,10} The presence of TLSs is closely correlated with a favorable prognosis and a positive response to immunotherapy in various types of cancer including BC,^{11–14} despite some controversy. Several studies have reported that the levels of tumor-infiltrating lymphocytes (TILs) and the presence of TLSs play valuable predictive roles in primary BC.^{15,16} However, our understanding of TLSs in BCBM tissues and their clinical relevance is limited.

Few studies have reported the role of the immune composition in BrMs owing to the scarcity of BrM samples. In this study, we evaluated the density, maturation, and composition of TLSs in BCBMs, established a novel TLS scoring system to quantify the abundance of TLSs in brain metastatic tumors, and elucidated their prognostic role using a patient cohort from Huashan Hospital, National Medical Center for Neurological Diseases of China. A multiplex immunofluorescence (mIF) assay was used to explore the heterogeneous immune composition of TLSs and explain their prognostic value, with the ultimate aim of contributing these findings to identify biological targets and guide future clinical trials.

MATERIALS AND METHODS

Patients and pathological evaluation of samples

Clinical and pathological data were collected from 98 patients with BCBM who underwent neurosurgery between 2015 and 2021 at Huashan Hospital of Fudan University. All the patients had pathologically confirmed BCBMs, diagnosed by two senior pathologists who were blinded to the study. Hormone receptor (HR) and HER2 statuses were assessed using immunohistochemical (IHC) staining or fluorescent in situ hybridization on paraffin-embedded tumor slides, following the guidelines of the American Society of Clinical Oncology/College of American Pathologists.^{17,18} Clinicopathological characteristics and treatment information of the BCBM patients are demonstrated in [table 1](#).

Examination and evaluation of TLSs

TLSs were assessed and quantified morphologically using H&E-stained specimens with a thickness of 4 μm, which were scanned into whole slide images (WSIs). Lymphoid

Table 1 Clinicopathological characteristics and treatment of the BCBM patients

		n	%
Age at time of BCBM	Mean	52 years	
	SD	10.3	
	Range	29–79 years	
Gender	Female	97	99.0
	Male	1	1.0
Breast cancer subtype of BM	TNBC	26	26.6
	HR+/HER2+	15	15.3
	HR+/HER2–	21	21.4
	HR–/HER2+	36	36.7
Number of BM sites	1	91	92.9
	2	5	5.1
	3 or more	2	2.0
KPS	90	31	31.6
	70–80	50	51.0
	60 or less	17	17.4
Metastatic sites	Frontal lobe	22	22.5
	Temporal lobe	11	11.2
	Parietal lobe	5	5.1
	Occipital lobe	11	11.2
	Cerebellum	32	32.7
	Others	17	17.3
De novo stage IV breast cancer	Yes	83	84.7
	No	15	15.3
Systemic therapy after BM diagnosis	Yes	84	85.7
	No	14	14.3
Radiotherapy after BM diagnosis	Yes	74	75.5
	No	24	24.5

BCBM, breast cancer brain metastases; HER2, human epidermal growth factor receptor 2; HR, hormone receptor; KPS, Karnofsky performance status; TNBC, triple-negative breast cancer.

aggregation with vessels exhibiting high endothelial venules features, with or without germinal centers, was considered TLSs.^{15,19} Two observers manually evaluated and annotated the abundance of TLSs in the intratumoral region of WSIs. The TLS scoring system used to quantify abundance was based on a previously described method.²⁰ Intratumoral TLSs density was categorized into four classes: score 0 indicated no typical TLSs in the area (TLS–); score 1 represented one or two TLSs; score 2 represented more than three TLSs distributed in the intratumoral area; and score 3 represented massive intratumoral TLSs converging with each other. Scores 1–3 were

considered TLS+. If there was a dispute over the scores, a third observer was consulted to reach a consensus.

Additionally, sections were stained with CD3, CD20, CD21, and CD23 antibodies to explore the maturation of TLSs and the presence of T lymphocytes, B cells, dendritic cells (DCs), and germinal center cells (GCs). TLSs with enriched CD20⁺ B cells and CD3⁺ T lymphocytes were recognized as being in the early TLS stage while primary follicle-like TLSs (CD20⁺ B cells and CD3⁺ T cell clusters, CD21⁺ DCs with CD23⁻) and secondary follicle-like TLSs (CD20⁺ B cells and CD3⁺ T cell clusters, CD21⁺ DCs with CD23⁺ GCs) were also classified.

Gene expression profiling

Two multigene expression signatures were used to detect the presence of TLSs, as previously reported.^{12 19 21} We examined the mRNA expression levels of CXCL9, CXCL10, CXCL11, CXCL13, CCL2, CCL4, CCL5, CCL8, CCL18, CCL19 and CCL21, then the expression levels of IGHG1, IGHM, IGKC, IGLC1, CD52, CD79A, MZB1, SSR4, XBP1, IL7R, CXCL12, LUM, C1QA, C7, APOE, PTGDS, PIM2 (some genes in the two signatures were not available in the arrays, such as CCL3). This analysis was performed by retrieving profile data from 32 BCM samples available in the Gene Expression Omnibus (accession numbers GSE2034 and GSE14020) and estimating them using the Affymetrix HT Human Genome U133A Array. Samples with a geometric mean higher than the third quartile were classified as TLS+ while those with a geometric mean lower than the third quartile were classified as TLS-.

mIF and cell percentage analyses

mIF staining was performed to elucidate the composition of spatially distinct TLSs using the iterative bleaching extended multiplexity (IBEX) method. This method involves several rounds of staining, imaging, and chemical bleaching, which are repeated as per the IBEX protocol.^{22 23} IBEX enables high-resolution imaging of over 65 parameters in the same tissue section without physical degradation, addressing the major limitation of capturing only a limited number of molecular features.

Briefly, formalin-fixed paraffin-embedded slides of 4 μm thickness were deparaffinized at 60°C for 1 hour and rehydrated in gradient alcohol. Slides were then blocked with 10% goat serum for 30 min at room temperature. Following this, fluorescence-conjugated primary antibodies were incubated overnight at 4°C. The antibodies used for staining are listed in online supplemental table S1. DAPI was employed as a nuclear counterstain. The sections were imaged using PhenoImager HT (AKOYA bioscience). The slides were then incubated with a 1 mg/mL LiBH₄ solution in diH₂O for fluorophore bleaching. The next panel of antibodies was added, and the procedure was repeated.

We used the commercially available Imaris software (Imaris x64 9.9.0) to calibrate, stitch and register the raw images. The final images were analyzed using the

QuPath V.0.5.0 image analysis software (Queen's University of Belfast, UK). Threshold values for each marker were applied to the scanning data to filter the positive cells. Additionally, cells that were positive for two markers simultaneously and above the cut-off value were defined as double-positive cells. Distinct cellular subgroups were enumerated by counting the number of stained cells per square millimeter and calculating the proportion of cells exhibiting positive staining among the DAPI-positive cells.²⁴ Owing to technical limitations, CD3⁺CD8⁺FoxP3⁺ cells were classified as regulatory T (Treg) cells, and CD3⁺CD8⁺PD-1⁺ cells as T follicular helper (Tfh) cells, based on previous studies.^{25–27} Furthermore, cell populations including CD68⁺CD163⁺ M2 macrophages, CD8⁺TIM-3⁺ T cells, CD8⁺ T lymphocytes, and CD68⁺PD-L1⁺ macrophages were identified.

Statistical analysis

The results are presented as mean±SD. Statistical analyses were performed using PRISM V.10, SPSS V.22.0, and R software V.4.2.2. A two-tailed t-test was used to compare quantitative data between the two groups, with $p < 0.05$ set as the threshold for significance. Qualitative variables were compared using the χ^2 test. Survival curves were generated using the Kaplan-Meier method and differences among patient subgroups were assessed using the log-rank test, with statistical significance set at $p < 0.05$.

Univariate and multivariate analyses were performed using the Cox proportional hazards regression model. Progression-free survival (PFS) was defined as the period between the date of diagnosis and disease progression (local, craniospinal, or extraneural) or death.²⁸ Disease progression was defined according to the Response Evaluation Criteria in Solid Tumors as a minimum 20% increase in the sum of the maximum tumor diameters, the appearance of new lesions, or an explicit advance in non-measurable malignant disease.²⁹ OS was evaluated from the date of surgery until death or last follow-up.³⁰

Nomograms containing the TLS score and other clinicopathological predictors were developed to predict the 1-year, 3-year, and 5-year OS and PFS using of “rms” and regplot R packages. Time-dependent ROC curves were plotted to estimate the predictive accuracy of the nomograms. Patients were classified into low or high nomoRiskScore groups based on the optimal cut-off value determined by the “survminer” R package.

RESULTS

Clinicopathological characteristics of patients

This study included 98 patients diagnosed with BCM who underwent neurosurgery between 2015 and 2021 at Huashan Hospital. The clinicopathological characteristics of the patients are shown in table 1. Variables included age, sex, BC subtype, number of BrM sites, Karnofsky performance status (KPS), metastatic sites in the brain, and presence or absence of comprehensive treatment.

The median age at diagnosis of BC and BCBM was 47 years (range, 25–74 years) and 52 years (range, 29–79 years), respectively. The median duration between BC diagnosis and BCBM occurrence was 37 months. Among the cases, TNBC subtype accounted for 26 patients (26.6%), HR+/HER2- subtype for 21 patients (21.4%), and HER2+ subtype for 51 patients (52.0%). Of the cases with available HR and HER2 status assessments of primary BC, 13 (17.3%) showed discordance in HR or HER2 status. Discordance in HR status was observed in 10.7% of patients with BCBM (n=8), where four lost HR expression while the other four gained it. Similarly, six patients (8%) showed an acquisition of HER2 expression on BCBM evaluation compared with their primary BC. The switch in HR and HER2 status between available primary BC and BCBM is shown in online supplemental figure S1. The majority of patients had de novo stage IV BC (84.7%) and a single BrM site (92.9%). BrM sites were most frequently located in the cerebellum (32.7%), consistent with a previous study.³¹ Most patients (82.6%) had a KPS score >70 points. After surgery, a large proportion of the patients underwent systemic therapy (85.7%) or radiotherapy (75.5%).

Density and maturation of TLSs in BCBMs

Intratumor TLSs were evaluated using WSIs stained with H&E. TLSs were observed in 47 patients and often demonstrated an irregular appearance. TLSs abundance was rated based on the scoring system described above. Representative images are shown in [figure 1A](#). Among the 47 patients, 16 (16.33%) scored 1, 17 (17.35%) scored 2, and 14 (14.29%) scored 3 ([figure 1B,C](#)). Besides, two previously reported multigene expression signatures were tested and used to confirm the existence of TLSs in metastatic brain lesions of BC patients ([figure 1D](#)). Previous studies have suggested that the stage of TLSs maturation may influence prognosis, potentially leading to different outcomes.^{13,32} To evaluate the organization and maturation of TLSs, IHC assays were conducted. As shown in [figure 2](#), CD3⁺ T lymphocytes and CD20⁺ B cells were the predominant components of TLSs. Interestingly, only 1 case out of 47 cases demonstrated primary follicle-like TLSs characterized by dense lymphocytic aggregates with a mixture of B and T cells and CD21 expression, but lacking CD23 expression. Secondary follicle-like TLSs containing CD23⁺ GCs were not observed in any of the examined cases.

Correlations between the abundance of TLSs and the clinical outcomes of BCBMs

We further explored the correlations between TLSs abundance and patient outcomes. With a median follow-up of 36.8 months from the diagnosis of BrM, 45 patients died, and 65 patients experienced disease progression. The TLS+ group exhibited superior OS and PFS compared with the TLS- group ([figure 3A,B](#), $p<0.001$). Additionally, there was a significant association between higher TLS scores and improved long-term survival ($p=0.003$) as well

as reduced disease progression ([figure 3C,D](#), $p<0.001$). Prognosis improved progressively with increasing TLS scores.

Given the known molecular subtype disparity in BC prognosis,³³ we evaluated the association between the BCBM subtype and outcome following BrM diagnosis and found significant differences between molecular subtype groups (online supplemental figure S2). KPS and de novo/relapsed stage IV BC were also significantly associated with survival outcome (univariate and multivariate analyses are listed in online supplemental tables S2–3). Subsequent analyses were performed separately for each subtype. Our findings revealed that within our cohort, the presence of TLSs was positively associated with OS ($p=0.0172$) and PFS ($p=0.0161$) in the HER2+ subtype ([figure 3E,F](#)), and prolonged OS ($p=0.0482$) in the TNBC subtype ([figure 3H,I](#)).

These results suggest that TLSs abundance can be used as a distinct prognostic stratification tool for patients with BCBM.

An intratumor TLS nomogram predicts BCBM prognosis

In previously published nomograms, variable screening was usually based on clinical evidence and statistical significance.³⁴ Based on these studies, we developed a graphical nomogram to estimate the 1-year, 3-year, and 5-year OS and PFS of patients with BCBM, considering various factors such as age, subtype, TLS score, KPS, de novo/relapsed stage IV BC diagnosis, and comprehensive treatment. Each grade of these variables was assigned a specific point on the scale, and the cumulative score for each patient was determined by adding the scores for all variables.

The presence of TLSs was identified as one of the three significant variables in the nomogram ([figure 4A](#)). A correlation was observed between decreased OS and elevated risk score associated with TLSs ([figure 4B](#), $p<0.001$). The AUC of the time-dependent ROC curve demonstrated favorable discrimination of the OS prediction nomogram ([figure 4](#), 1-year AUC=0.881, 3-year AUC=0.903, and 5-year AUC=0.817). Similarly, the nomogram for predicting PFS ([figure 4D](#)) revealed a significant association between a low-risk score and improved PFS ([figure 4E](#), $p<0.001$). The AUC exceeded 0.80 ([figures 4F](#), 1-year AUC=0.842, 3-year AUC=0.837, and 5-year AUC=0.807).

These findings reveal the prognostic ability of TLSs in BCBMs and the predictive ability of nomograms incorporating TLSs, enabling the recognition of high-risk patients with poor survival and disease progression.

Immune composition in TLSs assessed by mIF

To clarify the mechanisms responsible for the predictive significance of TLSs, a comprehensive understanding of the cellular composition and its impact on antitumor immune responses was necessary. We obtained 22 BCBM samples and observed the immune cell composition of the TLSs, comprising at least three representative samples

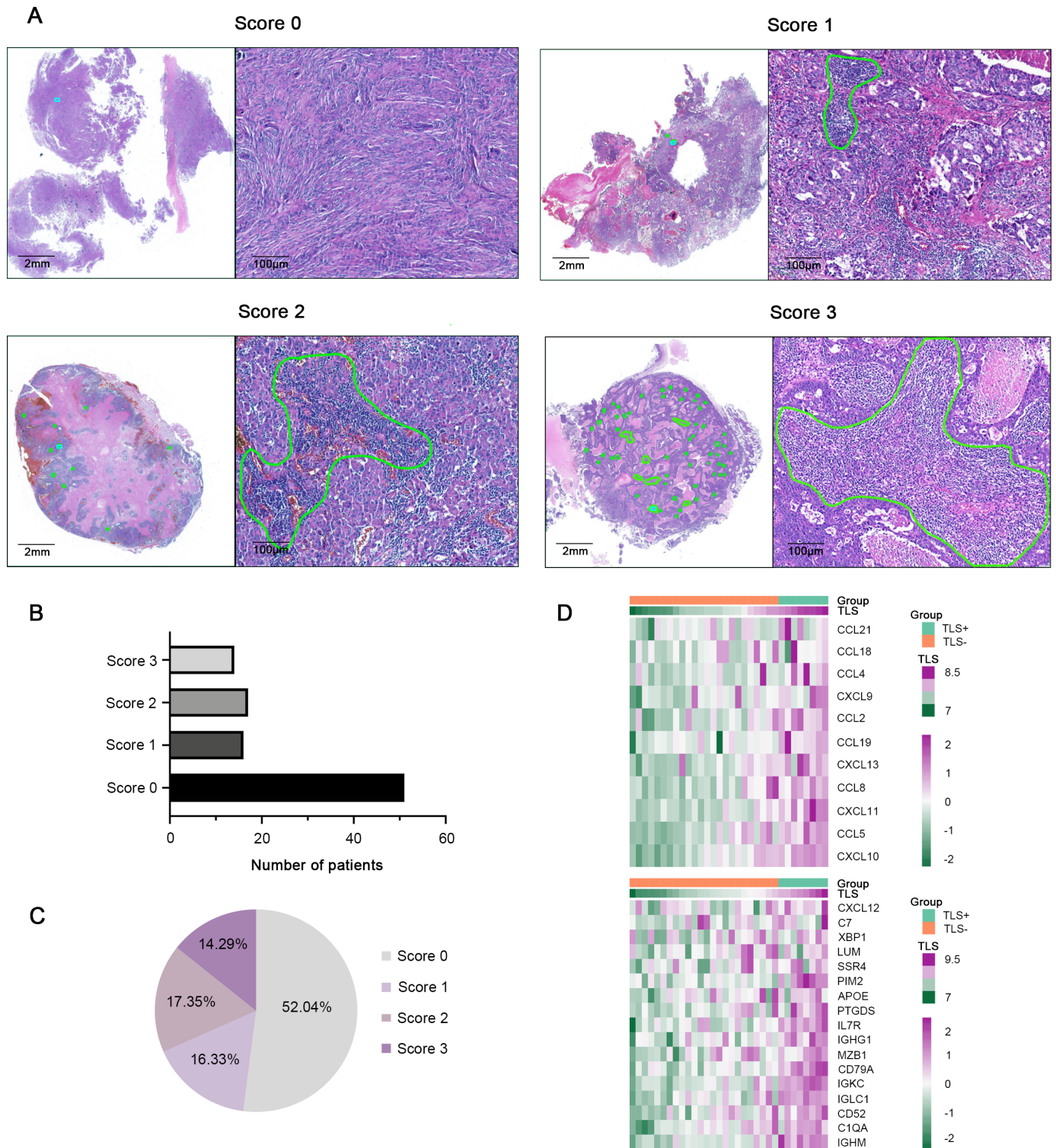


Figure 1 Characteristics and density of TLS in BCBMs. (A) Representative images of H&E staining for TLS scoring system (scores 0–3). TLSs are highlighted in green. (B, C) The number and percentage of scores 0–3 of TLS in all cases was determined. (D) Heat map of TLS relative gene expression in GSE2034 and GSE14020. BCBM, breast cancer brain metastases; TLS, tertiary lymphoid structure.

with scores of 0–3. The IBEX method, involving multiple rounds of staining, was used on the slides to visualize several different primary antibody stains. The representative images of mIF are shown in [figure 5A](#) and online supplemental figure S3. We then assessed the percentage

of infiltrating immune cells, including CD8⁺ cytotoxic T lymphocytes, CD3⁺CD8⁺PD-1⁺ Tfh cells, CD3⁺CD8⁺Foxp3⁺ Treg cells, CD68⁺CD163⁺ M2 macrophages, CD68⁺PD-L1⁺ PD-L1⁺ macrophages, and CD8⁺TIM-3⁺ T lymphocytes, which can elicit inflammatory or immunosuppressive

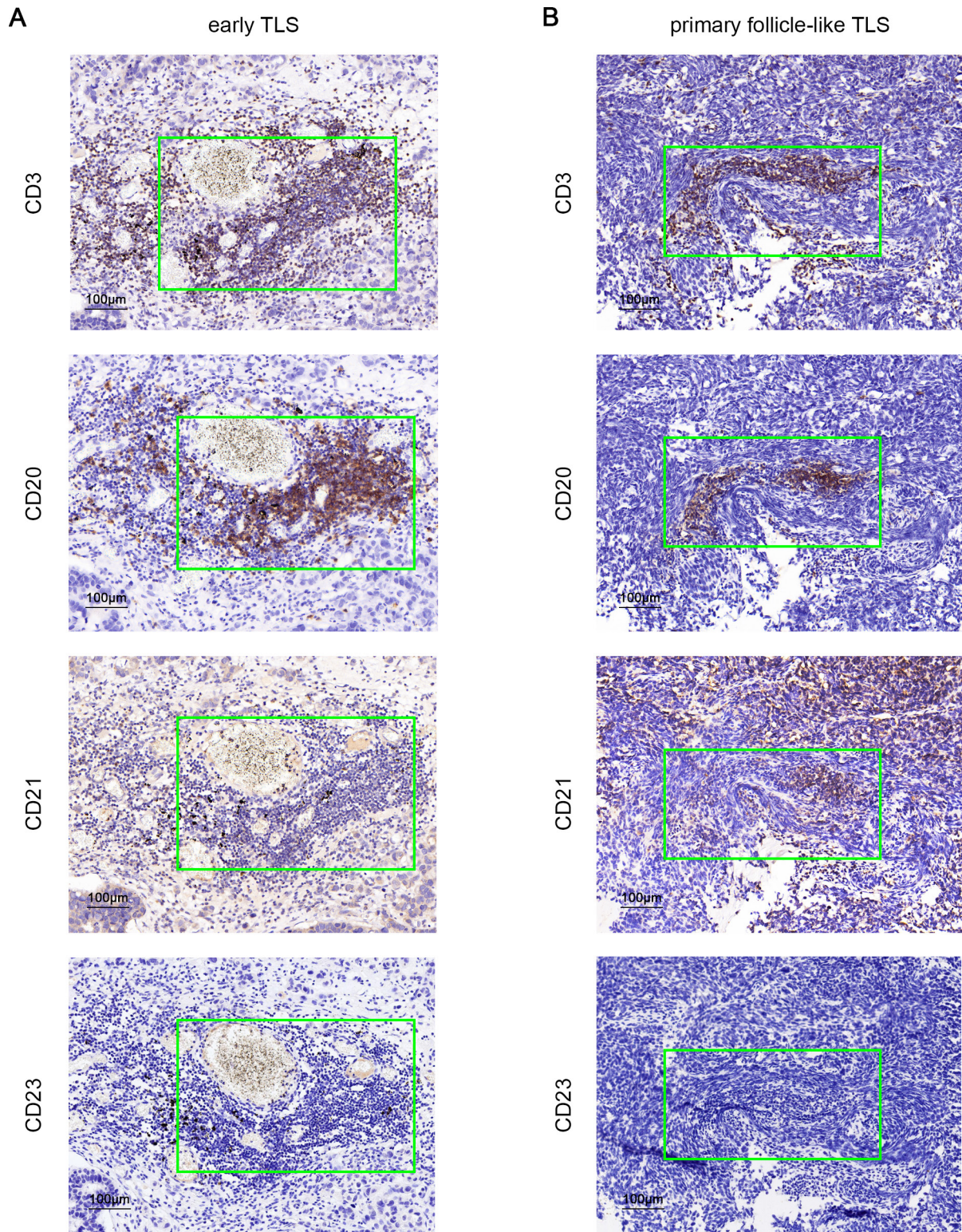


Figure 2 Characteristics of TLSs maturation heterogeneity in BCBMs. IHC assay to evaluate aggregates of lymphocytes that have histological features analogous to lymphoid tissues with CD3⁺ T cells, CD20⁺ follicular B cells, CD21⁺ follicular DCs, or CD23⁺ germinal center cells in serial sections. (A) Representative images of early TLSs. (B) Representative images of primary follicle-like TLSs. BCBM, breast cancer brain metastases; CD, cluster of differentiation; DC, dendritic cells; IHC, immunohistochemistry; TLS, tertiary lymphoid structure.

responses during tumor progression. The percentages of cytotoxic T lymphocytes, Tfh cells, M2 macrophages, and CD8⁺TIM-3⁺ T lymphocytes were significantly different

between the groups with scores of 0–3 (figure 5B; cytotoxic T lymphocytes, $p=0.044$; Tfh, $p=0.021$; M2 macrophages, $p=0.033$; CD8⁺TIM-3⁺ T lymphocytes, $p=0.018$).

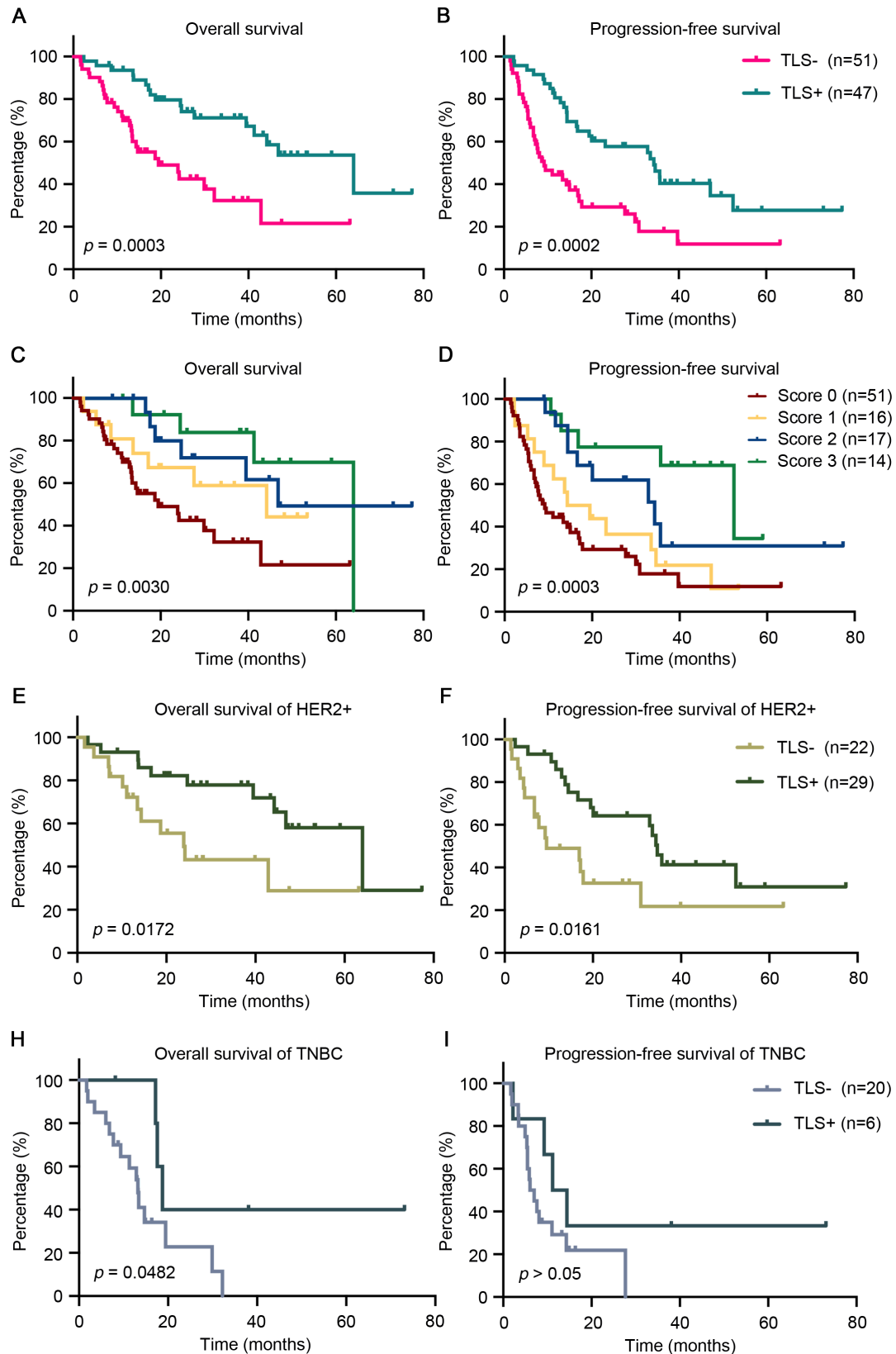


Figure 3 Prognostic value of TLSs presence and density in BCBM patients and correlation between TLSs and different breast subtype. (A, B) Kaplan-Meier and log-rank tests identifying the predictive value of the presence of TLSs for OS and PFS. (C, D) Kaplan-Meier curves showing OS and PFS of BCBM patients stratified by TLS scores. (E, F) Kaplan-Meier curves for OS and PFS in the HER2+ subtype according to the presence of TLSs. (H, I). Kaplan-Meier curves for OS and PFS in the TNBC subtype according to the presence of TLSs. BCBM, breast cancer brain metastases; HER2, human epidermal growth factor receptor type 2; OS, overall survival; PFS, progression-free survival; TLS, tertiary lymphoid structure; TNBC, triple-negative breast cancer.

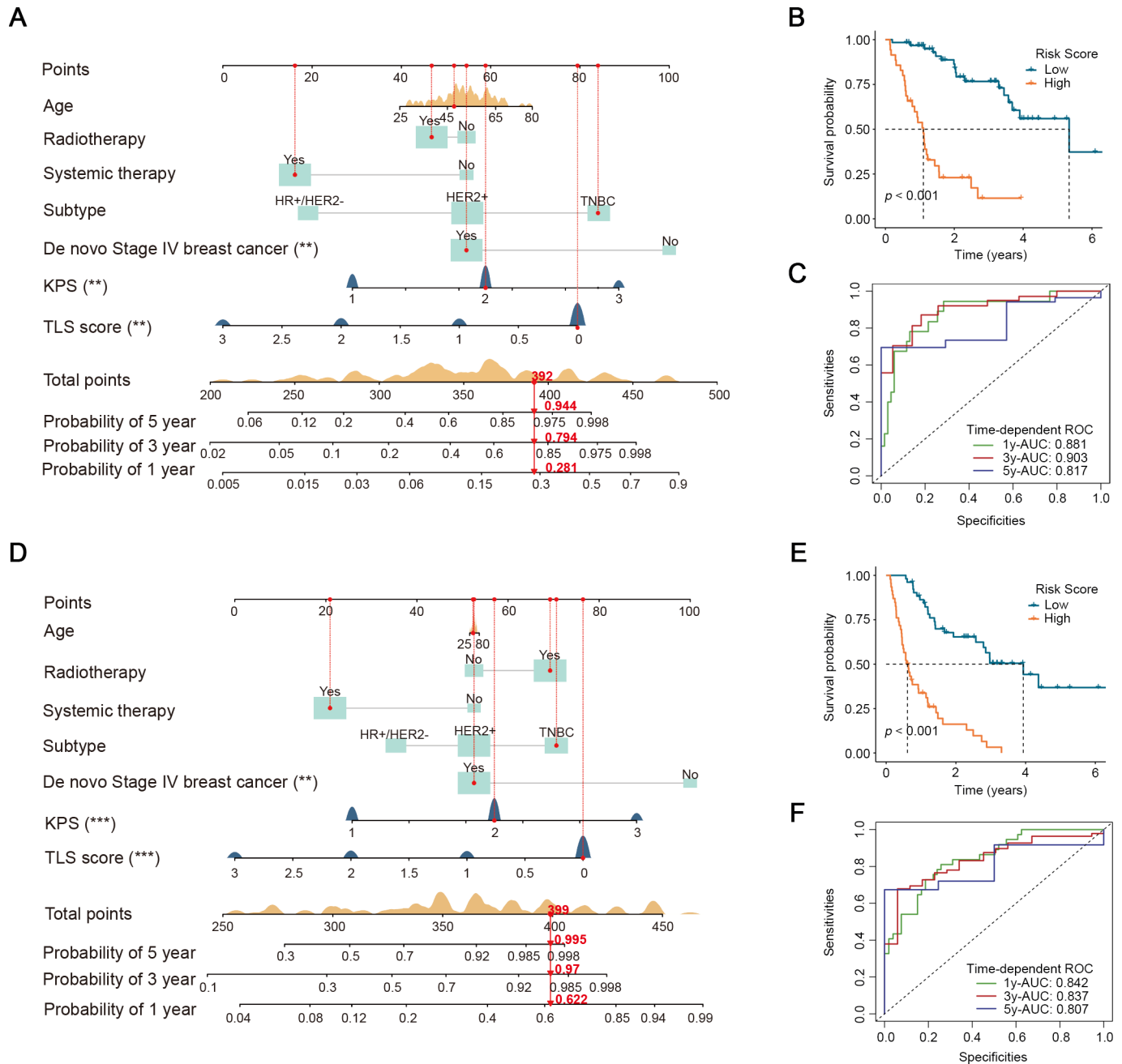


Figure 4 An intratumoral TLS nomogram predicts clinical outcome of BCBMs. (A–C) A TLS nomogram was established to predict the probability of 1-year, 3-year, and 5-year overall survival using Kaplan-Meier and ROC analyses. (D–E) A TLS nomogram was constructed to predict the probability of 1-year, 3-year, and 5-year progression-free survival using Kaplan-Meier and ROC analyses. AUC, area under the curve; BCBM, breast cancer brain metastases; KPS, Karnofsky performance status; ROC, receiver operating characteristic; TLS, tertiary lymphoid structure; **, $p < 0.01$; ***, $p < 0.001$.

The percentage of PD-L1⁺ macrophages within intratumoral TLSs remained consistently high across scores ranging from 1 to 3, although no significant differences were observed.

These findings provide insights into the diverse nature of the antitumor immune response and immunosuppressive effects induced by intratumoral TLSs of varying densities.

DISCUSSION

Over the past few decades, increasing evidence has emphasized that tumor immune infiltrates of metastatic BC strongly influence response to cancer therapies. Some BC subtypes were previously considered non-immunogenic; however, certain immune cell infiltrates may have prognostic value.³⁵ Recently, a series of studies has shown that TLSs can predict clinical outcomes and responses to immune checkpoint inhibitors in various cancer types.³² This study comprehensively evaluated the morphological and histological characteristics of TLSs in

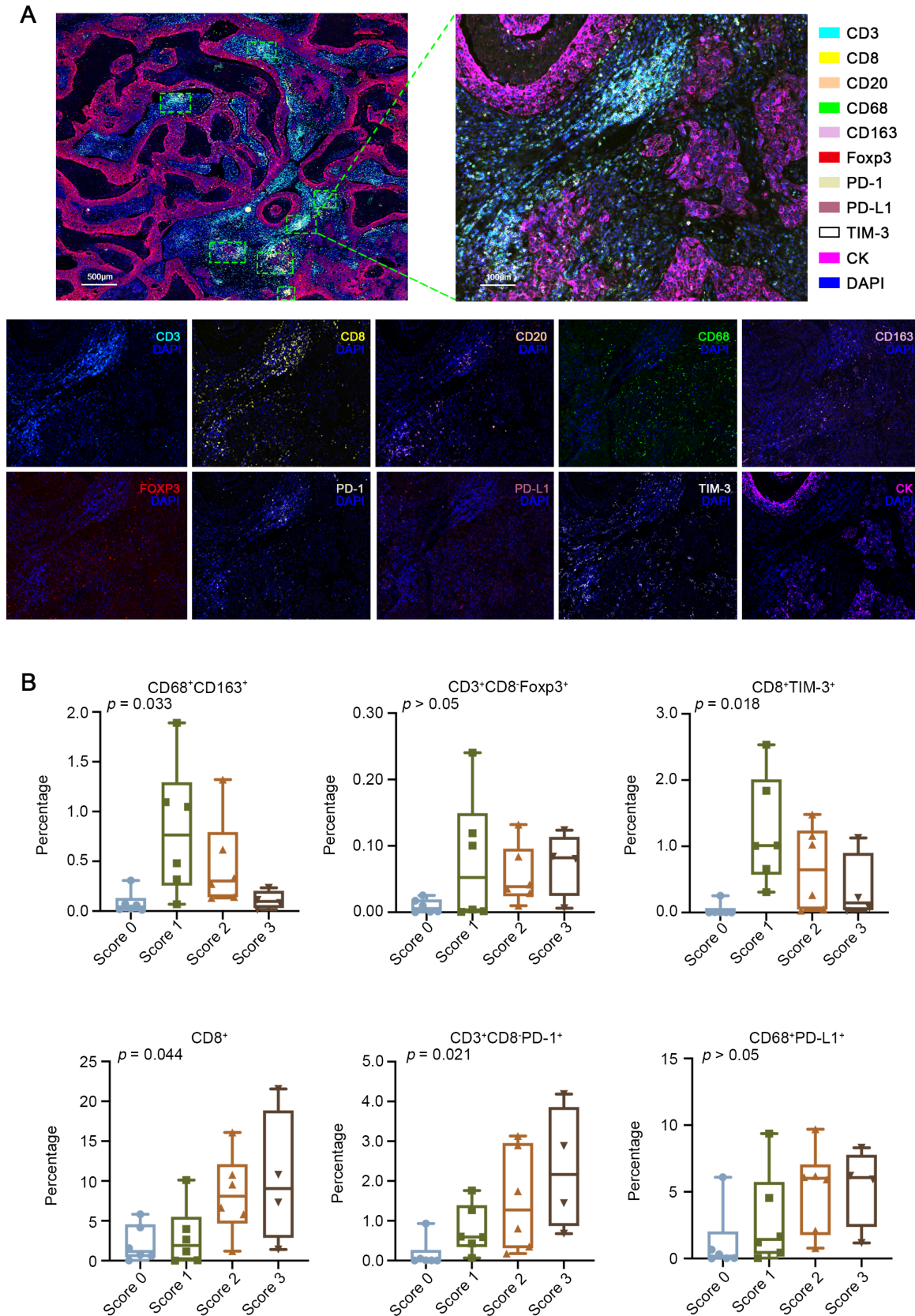


Figure 5 The heterogeneous distribution of immune cells within TLSs. (A) Representative multiplex immunofluorescence images showing the positivity of CD3, CD8, CD20, CD68, CD163, Foxp3, PD-1, PD-L1, TIM-3, and CK in intratumoral TLSs. (B) Comparison of the percentage of specific cell types among DAPI-positive cells using one-way ANOVA. ANOVA, analysis of variance; CD, cluster of differentiation; CK, cytokeratin; DAPI, 4',6-diamidino-2-phenylindole; PD-1, programmed cell death protein 1; PD-L1, programmed death-ligand 1; TIM-3, T cell immunoglobulin domain and mucin domain-3; TLS, tertiary lymphoid structure.

surgically resected BCBM, revealing their heterogeneity. By analyzing the clinical information of these cases, we described the association between TLSs abundance and patient prognosis. Furthermore, the mIF technique allowed us to determine the spatial immune cell composition and underlying antitumor immune responses of TLSs in BCBMs, which is challenging to evaluate using traditional immunohistochemistry or multigene sequencing techniques. Additionally, we constructed nomograms to predict the OS and PFS of patients with BCBM, demonstrating the predictive ability of incorporating TLSs and enabling the recognition of high-risk patients with poor outcomes.

Our study initially described the histological characteristics of TLSs and demonstrated their complex roles based on the abundance in patients with BCBM. Several previous studies have outlined a TLS scoring system for the density and three maturation stages of the TLSs in different carcinomas, including primary BC.^{20 32 36} However, the assessment of TLSs in metastatic BC tumors is rare. A recent report suggested the absence of TLSs in the brain metastases of BC and proposed that the presence of TLSs in primary BC tumors might influence this absence; however, the sample size was small.³⁷ Another study found that tumors originating in the brain altered their TME differently compared with cancers that metastasizing from extracranial organs, reflecting greater immune cell diversity in BrMs.³⁸ In our study, TLSs were found in 47 cases, and IHC was conducted to verify their existence and assess their maturation. We observed that most TLSs in BCBM exhibited characteristics of early TLSs (dense lymphocytic aggregates with mixed B and T cells, without CD21 or CD23 expression), and only one case demonstrated primary follicle-like TLSs (dense lymphocytic aggregates with mixed B and T cells, CD21 expression, and negative CD23). This result is consistent with the findings reported by Masuda *et al.*, indicating the absence of primary or secondary follicle-like TLSs in kidney clear cell carcinoma.³⁹ Previous studies have suggested that TLSs in some primary tumors exhibit a low proportion of primary and secondary follicle-like TLSs.²⁴ This may be due to the time required for TLS maturation, whereas metastatic lesions in the brain tend to grow rapidly and develop into severe symptoms. Moreover, piecemeal resections in some cases may result in fragmented pathological samples, increasing the difficulty of assessment.⁴⁰ To the best of our knowledge, this study is a pioneering effort to uncover the existence and maturation of TLSs in metastatic brain lesions of BC patients, confirmed by previously reported multigene expression signatures (figure 1D).

Additionally, the favorable prognosis of patients was significantly correlated with a higher density of intratumoral TLSs, although the exact mechanism remains unclear. In our study, positive intratumoral TLSs and higher TLS scores indicated better OS and PFS. This finding aligns with previous understandings of TLSs in other cancer types¹⁹ and metastatic tumors.⁴¹ The BC

subtype is often considered an important indicator of clinical outcomes in patients with BC. In this study, the BC subtype was identified as a clinical variable influencing prognosis following BrM diagnosis, along with other well-established prognostic factors such as KPS. Despite the discordance in HR or HER2 status between primary BC and BCBM, reported in previous studies,⁴² we explored the prognostic role of TLSs in different BCBM subtypes. The results showed that TLS presence was positively associated with OS and PFS in the HER2+ subtype and with prolonged OS in the TNBC subtype. This aligns with the commonly accepted notion that immune cell infiltration and TLSs in patients diagnosed with primary TNBC and HER2+BC correlate with improved prognosis.^{15 43 44} Nevertheless, some studies have pointed out that tumor-proximal TLSs and tumor-distal TLSs exhibit opposing prognostic trends in several cancer types.^{20 39} However, it is difficult to evaluate the condition of tumor-distal TLSs in intracranial metastatic lesions because of the limitations of brain tumor resection.

Furthermore, mIF staining was used to assess the immune composition of TLSs and elucidate differences between the score 0–3 groups. M2 macrophages possess tumor-supporting abilities, including angiogenesis and neovascularization.⁴⁵ The percentage of CD68⁺CD163⁺ M2 macrophages decreased significantly in the score 3 TLS group, and CD3⁺CD8⁺Foxp3⁺Treg cells also showed a declining trend, indicating a potential negative correlation between TLSs density and the immunosuppressive microenvironment. However, the percentage of CD3⁺CD8⁺PD-1⁺ Tfh cells was positively correlated with TLSs abundance. Tfh cells are known to promote antitumor immune responses in BC,⁴⁶ and a high number of Tfh cells may indicate a favorable prognosis for patients with BCBM. Meanwhile, as an effector and indicator of antitumor immunity and responses,⁴⁷ the increasing percentage of CD8⁺ T cells suggested elevated antitumor immunity in the score three group. Additionally, the reduction in CD8⁺TIM-3⁺ T cells was accompanied by an increase in TLS density. The role of CD8⁺TIM-3⁺ T cells in BCBMs with TLSs requires further exploration, as TIM-3 expression on CD8⁺ T cells in the TME is usually considered a sign of T cell dysfunction.⁴⁸ TIM-3-targeted immunotherapies may enhance the response to checkpoint blockade.⁴⁹ Furthermore, the markers of antigen presenting cells, natural killer cells, tumor proliferation and apoptosis, such as HLA-I, HLA-II, CD57, cleaved Caspase-3 and Ki-67, together with CXCR5, TCF-1, BCL-6, CD4, CD8, CD20, and CK, were stained in TLS-positive samples. Due to technical limitations, the results showed the distribution of these cells (online supplemental figure S3), and we hope to analyze the differences of these immune compositions related to TLSs density in BCBM in a future research. Collectively, these findings may explain the correlations between TLSs and prognosis in BCBMs to some degree, and the distinct immune composition of TLSs may exhibit either tumor-promoting or tumor-inhibiting effects.

This study has several limitations. First, the sample size was limited to a single center due to the rarity of the disease. Second, because many BC patients received treatment at other medical institutions before developing brain metastases, we faced challenges in investigating the clinicopathological characteristics and treatment information of primary BC. Third, piecemeal resections in some cases made histological assessment difficult, although en bloc resection samples were included whenever possible. Moreover, the predictive value of TLS for immune checkpoint inhibitor responses in patients with BCBM has not been explored. Additionally, the mechanisms by which TLSs abundance or maturation affects abnormal TME phenotypes has not yet been investigated, despite TLS-induced therapy being considered a promising cancer treatment strategy.⁵⁰ Therefore, a multicenter prospective study using patient-derived tumor xenograft models would be valuable for verifying the findings of our study.

In summary, despite the limitations of the study's retrospective nature and limited sample size, this research represents the most comprehensive analysis of TLSs in BCBMs to date, focused on prognosis. Our study highlights the predictive value of intratumoral TLS, which is closely correlated with BC subtype. Moreover, we demonstrated the specific cellular composition of TLSs, which may increase confidence in the response to immunotherapy and TLS-induced treatment strategies in BCBM.

Author affiliations

¹Department of General Surgery, Huashan Hospital, Shanghai Medical College, Fudan University, Shanghai, China

²Department of Neurosurgery, Huashan Hospital, Shanghai Medical College, Fudan University, Shanghai, China

³Research Unit of New Technologies of Micro-Endoscopy Combination in Skull Base Surgery (2018RU008), Chinese Academy of Medical Sciences, Beijing, China

⁴National Center for Neurological Disorders, Shanghai, China

⁵Shanghai Key Laboratory of Brain Function Restoration and Neural Regeneration, Shanghai, China

⁶Neurosurgical Institute of Fudan University, Shanghai, China

⁷Shanghai Clinical Medical Center of Neurosurgery, Shanghai, China

⁸Department of Pathology, Huashan Hospital, Shanghai Medical College, Fudan University, Shanghai, China

Correction notice This article has been corrected since it was first published. It has now been indicated that Y-YZ, ZF and B-RT contributed equally.

Acknowledgements We thank all who participated in this study and extend our special appreciation to Dr Shi-Zhe Yu for his technical support in performing multiplex immunofluorescence.

Contributors All authors made contributions to the conception and design of the study. Material preparation and data collection were performed by YYZ and ZF. Data analysis was conducted by BRT. Pathological assessment was verified by ZGD. The first draft of the manuscript was written by YYZ and revised by ZF and ZFS. YYZ is the guarantor.

Funding This work was supported by the grants from National Natural Science Foundation of China (No. 82203789) and CAMS Innovation Fund for Medical Sciences (CIFMS, 2019-I2M-5-008).

Competing interests No, there are no competing interests.

Patient consent for publication Not applicable.

Ethics approval This study involves human participants and was approved by the ethical committee/institutional review board of Huashan Hospital of Fudan University (No. 2015-256). Participants gave informed consent to participate in the study before taking part.

Provenance and peer review Not commissioned; externally peer reviewed.

Data availability statement Data are available on reasonable request. The data that support the findings of this study are available from the corresponding author on reasonable request.

Supplemental material This content has been supplied by the author(s). It has not been vetted by BMJ Publishing Group Limited (BMJ) and may not have been peer-reviewed. Any opinions or recommendations discussed are solely those of the author(s) and are not endorsed by BMJ. BMJ disclaims all liability and responsibility arising from any reliance placed on the content. Where the content includes any translated material, BMJ does not warrant the accuracy and reliability of the translations (including but not limited to local regulations, clinical guidelines, terminology, drug names and drug dosages), and is not responsible for any error and/or omissions arising from translation and adaptation or otherwise.

Open access This is an open access article distributed in accordance with the Creative Commons Attribution Non Commercial (CC BY-NC 4.0) license, which permits others to distribute, remix, adapt, build upon this work non-commercially, and license their derivative works on different terms, provided the original work is properly cited, appropriate credit is given, any changes made indicated, and the use is non-commercial. See <http://creativecommons.org/licenses/by-nc/4.0/>.

ORCID iD

Zhen Fan <http://orcid.org/0009-0007-9257-0201>

REFERENCES

- Morgan AJ, Giannoudis A, Palmieri C. The genomic landscape of breast cancer brain metastases: a systematic review. *Lancet Oncol* 2021;22:e7–17.
- Nayak L, Lee EQ, Wen PY. Epidemiology of brain metastases. *Curr Oncol Rep* 2012;14:48–54.
- Darlix A, Louvel G, Fraisse J, et al. Impact of breast cancer molecular subtypes on the incidence, kinetics and prognosis of central nervous system metastases in a large multicentre real-life cohort. *Br J Cancer* 2019;121:991–1000.
- Onkar SS, Carleton NM, Lucas PC, et al. The great immune escape: understanding the divergent immune response in breast cancer subtypes. *Cancer Discov* 2023;13:23–40.
- Dutoit V, Migliorini D, Dietrich P-Y, et al. Immunotherapy of malignant tumors in the brain: how different from other sites? *Front Oncol* 2016;6:256.
- Goldberg SB, Gettinger SN, Mahajan A, et al. Pembrolizumab for patients with melanoma or non-small-cell lung cancer and untreated brain metastases: early analysis of a non-randomised, open-label, phase 2 trial. *Lancet Oncol* 2016;17:976–83.
- Trujillo JA, Sweis RF, Bao R, et al. T cell-inflamed versus non-T cell-inflamed tumors: a conceptual framework for cancer immunotherapy drug development and combination therapy selection. *Cancer Immunol Res* 2018;6:990–1000.
- Liu Y, Xun Z, Ma K, et al. Identification of a tumour immune barrier in the HCC microenvironment that determines the efficacy of immunotherapy. *J Hepatol* 2023;78:770–82.
- Sautès-Fridman C, Petitprez F, Calderaro J, et al. Tertiary lymphoid structures in the era of cancer immunotherapy. *Nat Rev Cancer* 2019;19:307–25.
- Schumacher TN, Thommen DS. Tertiary lymphoid structures in cancer. *Science* 2022;375:eabf9419.
- Cabrita R, Lauss M, Sanna A, et al. Tertiary lymphoid structures improve immunotherapy and survival in melanoma. *Nature New Biol* 2020;577:561–5.
- Meylan M, Petitprez F, Becht E, et al. Tertiary lymphoid structures generate and propagate anti-tumor antibody-producing plasma cells in renal cell cancer. *Immunity* 2022;55:527–41.
- Vanhersecke L, Brunet M, Guégan J-P, et al. Mature tertiary lymphoid structures predict immune checkpoint inhibitor efficacy in solid tumors independently of PD-L1 expression. *Nat Cancer* 2021;2:794–802.
- Fridman WH, Meylan M, Petitprez F, et al. B cells and tertiary lymphoid structures as determinants of tumour immune contexture and clinical outcome. *Nat Rev Clin Oncol* 2022;19:441–57.
- Lee HJ, Park IA, Song IH, et al. Tertiary lymphoid structures: prognostic significance and relationship with tumour-infiltrating lymphocytes in triple-negative breast cancer. *J Clin Pathol* 2016;69:422–30.
- Song IH, Heo S-H, Bang WS, et al. Predictive value of tertiary lymphoid structures assessed by high endothelial venule counts in

- the neoadjuvant setting of triple-negative breast cancer. *Cancer Res Treat* 2017;49:399–407.
- 17 Hammond MEH, Hayes DF, Dowsett M, et al. American society of clinical oncology/college of american pathologists guideline recommendations for immunohistochemical testing of estrogen and progesterone receptors in breast cancer. *J Clin Oncol* 2010;28:2784–95.
 - 18 Wolff AC, Hammond MEH, Allison KH, et al. Human epidermal growth factor receptor 2 testing in breast cancer: american society of clinical oncology/college of american pathologists clinical practice guideline focused update. *JCO* 2018;36:2105–22.
 - 19 Calderaro J, Petitprez F, Becht E, et al. Intra-tumoral tertiary lymphoid structures are associated with a low risk of early recurrence of hepatocellular carcinoma. *J Hepatol* 2019;70:58–65.
 - 20 Ding G-Y, Ma J-Q, Yun J-P, et al. Distribution and density of tertiary lymphoid structures predict clinical outcome in intrahepatic cholangiocarcinoma. *J Hepatol* 2022;76:608–18.
 - 21 Coppola D, Nebozhyn M, Khalil F, et al. Unique ectopic lymph node-like structures present in human primary colorectal carcinoma are identified by immune gene array profiling. *Am J Pathol* 2011;179:37–45.
 - 22 Radtke AJ, Kandov E, Lowekamp B, et al. IBEX: A versatile multiplex optical imaging approach for deep phenotyping and spatial analysis of cells in complex tissues. *Proc Natl Acad Sci U S A* 2020;117:33455–65.
 - 23 Radtke AJ, Chu CJ, Yaniv Z, et al. IBEX: an iterative immunolabeling and chemical bleaching method for high-content imaging of diverse tissues. *Nat Protoc* 2022;17:378–401.
 - 24 Xu W, Lu J, Liu WR, et al. Heterogeneity in tertiary lymphoid structures predicts distinct prognosis and immune microenvironment characterizations of clear cell renal cell carcinoma. *J Immunother Cancer* 2023;11:e006667.
 - 25 Parra ER, Zhang J, Jiang M, et al. Immune cellular patterns of distribution affect outcomes of patients with non-small cell lung cancer. *Nat Commun* 2023;14:2364.
 - 26 Kumar T, Hobbs E, Yang F, et al. Tumor immune microenvironment changes by multiplex immunofluorescence staining in a pilot study of neoadjuvant talazoparib for early-stage breast cancer patients with a hereditary BRCA mutation. *Clin Cancer Res* 2022;28:3669–76.
 - 27 Andersen LB, Nørgaard M, Rasmussen M, et al. Immune cell analyses of the tumor microenvironment in prostate cancer highlight infiltrating regulatory T cells and macrophages as adverse prognostic factors. *J Pathol* 2021;255:155–65.
 - 28 Gyawali B, Eisenhauer E, Tregear M, et al. Progression-free survival: it is time for a new name. *Lancet Oncol* 2022;23:328–30.
 - 29 Eisenhauer EA, Therasse P, Bogaerts J, et al. New response evaluation criteria in solid tumours. 2009.
 - 30 Gourgou-Bourgade S, Cameron D, Poortmans P, et al. Guidelines for time-to-event end point definitions in breast cancer trials: results of the DATECAN initiative (definition for the assessment of time-to-event endpoints in cancer trials). *Ann Oncol* 2015;26:2505–6.
 - 31 Travers SS, Fisher CM, Kabos P, et al. Breast cancer brain metastases localization and risk of hydrocephalus: a single institution experience. *J Neurooncol* 2023;163:115–21.
 - 32 Kinker GS, Vitiello GAF, Diniz AB, et al. Mature tertiary lymphoid structures are key niches of tumour-specific immune responses in pancreatic ductal adenocarcinomas. *Gut* 2023;72:1927–41.
 - 33 Peiffer DS, Zhao F, Chen N, et al. Clinicopathologic characteristics and prognosis of ERBB2-low breast cancer among patients in the national cancer database. *JAMA Oncol* 2023;9:500–10.
 - 34 Iasonos A, Schrag D, Raj GV, et al. How to build and interpret a nomogram for cancer prognosis. *J Clin Oncol* 2008;26:1364–70.
 - 35 Tien TZ, Lee JNLW, Lim JCT, et al. Delineating the breast cancer immune microenvironment in the era of multiplex immunohistochemistry/immunofluorescence. *Histopathology* 2021;79:139–59.
 - 36 Wang Q, Sun K, Liu R, et al. Single-cell transcriptome sequencing of B-cell heterogeneity and tertiary lymphoid structure predicts breast cancer prognosis and neoadjuvant therapy efficacy. *Clin Transl Med* 2023;13:e1346.
 - 37 Lee M, Heo SH, Song IH, et al. Presence of tertiary lymphoid structures determines the level of tumor-infiltrating lymphocytes in primary breast cancer and metastasis. *Mod Pathol* 2019;32:70–80.
 - 38 Klemm F, Maas RR, Bowman RL, et al. Interrogation of the microenvironmental landscape in brain tumors reveals disease-specific alterations of immune cells. *Cell* 2020;181:1643–60.
 - 39 Masuda T, Tanaka N, Takamatsu K, et al. Unique characteristics of tertiary lymphoid structures in kidney clear cell carcinoma: prognostic outcome and comparison with bladder cancer. *J Immunother Cancer* 2022;10:e003883.
 - 40 Nahed BV, Alvarez-Breckenridge C, Brastianos PK, et al. Congress of neurological surgeons systematic review and evidence-based guidelines on the role of surgery in the management of adults with metastatic brain tumors. *Neurosurg* 2019;84:E152–5.
 - 41 Zhang C, Wang X-Y, Zuo J-L, et al. Localization and density of tertiary lymphoid structures associate with molecular subtype and clinical outcome in colorectal cancer liver metastases. *J Immunother Cancer* 2023;11:e006425.
 - 42 Hulsbergen AFC, Claes A, Kavouridis VK, et al. Subtype switching in breast cancer brain metastases: a multicenter analysis. *Neuro Oncol* 2020;22:1173–81.
 - 43 Loi S, Drubay D, Adams S, et al. Tumor-infiltrating lymphocytes and prognosis: a pooled individual patient analysis of early-stage triple-negative breast cancers. *J Clin Oncol* 2019;37:559–69.
 - 44 Liu X, Tsang JYS, Hlaing T, et al. Distinct tertiary lymphoid structure associations and their prognostic relevance in HER2 positive and negative breast cancers. *Oncologist* 2017;22:1316–24.
 - 45 Liu J, Geng X, Hou J, et al. New insights into M1/M2 macrophages: key modulators in cancer progression. *Cancer Cell Int* 2021;21:389.
 - 46 Noël G, Fontsa ML, Garaud S, et al. Functional th1-oriented T follicular helper cells that infiltrate human breast cancer promote effective adaptive immunity. *J Clin Invest* 2021;131:e139905.
 - 47 Giles JR, Globig AM, Kaech SM, et al. CD8+ T cells in the cancer-immunity cycle. *Immunity* 2023;56:2231–53.
 - 48 Dixon KO, Tabaka M, Schramm MA, et al. TIM-3 restrains anti-tumour immunity by regulating inflammasome activation. *Nature New Biol* 2021;595:101–6.
 - 49 Acharya N, Sabatos-Peyton C, Anderson AC. Tim-3 finds its place in the cancer immunotherapy landscape. *J Immunother Cancer* 2020;8:e000911.
 - 50 Johansson-Percival A, He B, Li ZJ, et al. De novo induction of intratumoral lymphoid structures and vessel normalization enhances immunotherapy in resistant tumors. *Nat Immunol* 2017;18:1207–17.